ACS APPLIED MATERIALS & INTERFACES

Research Article

www.acsami.org

Enhanced Photoanodic Output at an Organic p/n Bilayer in the Water Phase by Means of the Formation of Whiskered Phthalocyanine

Toshiyuki Abe,*[,†,‡] Yoshinori Tanno,[†,‡] Toshihiro Ebina,[†] Shouichi Miyakushi,[†] and Keiji Nagai[§]

[†]Department of Frontier Materials Chemistry, Graduate School of Science and Technology, Hirosaki University, 3 Bunkyo-cho, Hirosaki 036-8561, Japan

[§]Chemical Resources Laboratory, Tokyo Institute of Technology, Suzukake-dai, Midori-ku, Yokohama 226-8503, Japan

Supporting Information

ABSTRACT: The photoelectrode characteristics of an organic p/n bilayer in the water phase were studied with respect to film; 3,4,9,10-perylenetetracarboxylic-bisbenzimidazole (PTCBI, an n-type semiconductor) was used in combination with 29*H*,31*H*-phthalocyanine (H_2Pc, a p-type semiconductor). When H_2Pc was vapor-deposited on top of the PTCBI layer on a heated substrate (cf. degree of pressure, ca. 5.0×10^{-4} Pa; temperature at the substrate, 120°C), a transmission electron microscopic image showed an enhanced contact area of the p/n interface in comparison with that prepared at r.t., due to the formation of a whisker H_2Pc. The PTCBI/H_2Pc bilayer can work as a photoanode along with photophysical events in its interior. The rate-limiting charge transfer at the H_2Pc/water interface was kinetically analyzed assuming the Langmuir adsorption equilibrium at that interface. Kinetic analysis demonstrated that the increased contact area can successfully lead to efficient photoinduced carrier generation; particularly, when a thick whisker of H_2Pc was formed, the magnitude of the oxidation kinetics at the H_2Pc/water interface was approximately 2.5 times higher than that without thermal treatment.

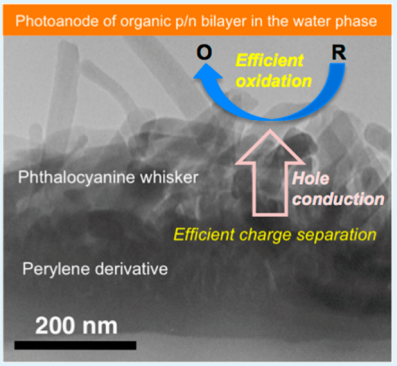

KEYWORDS: *organic p/n bilayer, perylene derivative, phthalocyanine, whisker, visible-light-responsive photoelectrode, photoelectrochemistry, Langmuir adsorption equilibrium*

INTRODUCTION

Organic semiconductors have attracted attention due to their low cost, great variety, processing ease, etc. Organic semiconductors have been applied to solar cells,[1−6] electroluminescent devices,[7−9] and field effect transistors.[10−12] Those applications have been researched and developed with the devices working in a dry state. Although organic p/n bilayers have been recognized as part of photovoltaic cells, we have also revealed their novel function as photoelectrodes in the water phase.[13−22] For example, the p-type conductor/water interface can induce oxidation along with photophysical events (i.e., visible light absorption, exciton formation, carrier generation at the p/n interface, and its conduction) in the p/n interior. Organic bilayers, capable of water oxidation and proton reduction into O_2,[14,15] and H_2,[22] respectively, have also been found. Such organo-photoelectrodes involve advanced and essential characteristics of photoenergy conversion, wherein wide visible-light energy is available for reaction at the solid/water interface. The photoelectrode kinetics of an organic p/n bilayer has been confirmed to be dominated by charge transfer at the solid/water interface,[16,17,19,21] distinct from the corresponding photovoltaic cell.[23,24] In the rate-limiting charge transfer reaction, photocurrents can be generated to be proportional to the surface concentrations of carrier and reactant. Therefore, in order to develop an efficient organic p/n bilayer photoelectrode, the p/n interface for carrier generation and/or the surface available for the charge transfer reaction need to be activated.

In the present work, some types of organic p/n bilayers, comprised of 3,4,9,10-perylenetetracarboxylic-bisbenzimidazole (PTCBI, an n-type semiconductor) and 29*H*,31*H*-phthalocyanine (H_2Pc, a p-type semiconductor), were prepared with and without thermal application during vapor deposition; that is, a trial was carried out to develop an efficient PTCBI/H_2Pc bilayer photoelectrode. Kinetic analysis for rate-limiting charge transfer was conducted with each bilayer, through which the correlation between the interfacial structures of the p/n bilayer and the photoanodic output at the H_2Pc surface was examined.

EXPERIMENTAL SECTION

Chemicals and Preparation Procedure of Organic p/n Bilayer. PTCBI was synthesized and purified according to a previously described procedure.[25] H_2Pc (Tokyo Chemical Industry Co., Ltd.) was commercially available and purified by sublimation prior to use [cf. thermal control was conducted for the exterior of the vessel (cf. temperature, 510°C; degree of pressure within the vessel, ca. 1×10^{-2} Pa)]. 2-Mercaptoethanol (RS^-) was obtained from Kanto Chemical Co., Inc. The indium−tin oxide (ITO)-coated glass plate (resistance, 8 $\Omega \cdot cm^{-2}$; transmittance, >85%; ITO thickness, 174 nm) was obtained from Asahi Glass Co., Ltd.

Received: October 4, 2012
Accepted: January 30, 2013
Published: January 30, 2013

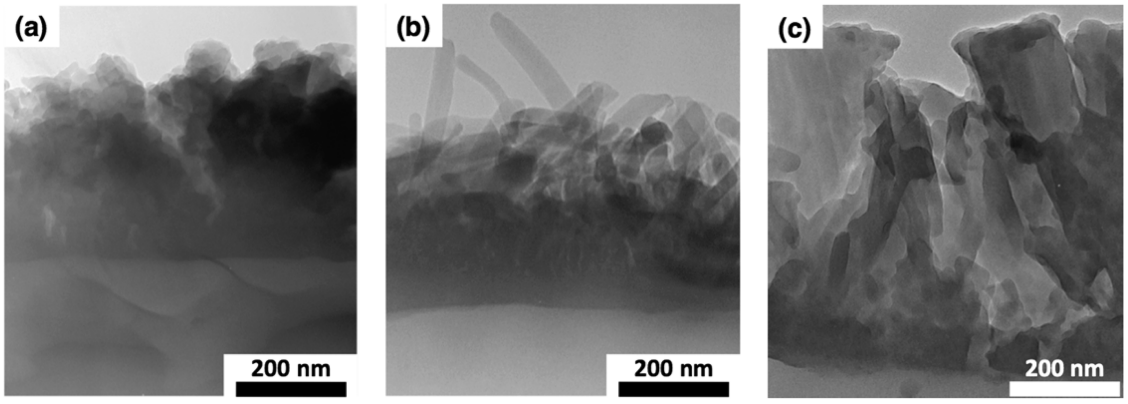

Figure 1. TEM images of ITO/PTCBI/H_2Pc-A (a), ITO/PTCBI/H_2Pc-B (b), and ITO/PTCBI/H_2Pc-C (c).

Three types of PTCBI/H_2Pc bilayers were prepared by vapor deposition (apparatus, ULVAC KIKO VPC-260; degree of pressure, ca. 5.0×10^{-4} Pa; deposition speed, 0.03 nm·s^{-1}). All the bilayers were composed of PTCBI coated on an ITO with H_2Pc coated on top of the PTCBI layer. The vapor deposition apparatus was equipped with a thermostat (Densei–Lambda Z-UP 10-40) to regulate the temperature of the ITO plate. When preparing the bilayers, thermal control was conducted as follows: (i) the PTCBI/H_2Pc bilayer was fabricated at r.t. (denoted as ITO/PTCBI/H_2Pc-A); (ii) after coating PTCBI on an ITO at r.t., H_2Pc was deposited at 120°C (denoted as ITO/PTCBI/H_2Pc-B); (iii) the resulting ITO/PTCBI/H_2Pc-B was cooled to r.t., followed by further deposition of H_2Pc at r.t. (denoted as ITO/PTCBI/H_2Pc-C). The temperature employed in (ii) was selected since the sublimation of H_2Pc can also start to take place at the substrate, particularly at temperatures higher than 120°C (degree of pressure, ca. 5.0×10^{-4} Pa). The deposited amount was monitored through a quartz microbalance (ULVAC, CRTM-6000) equipped with a vapor deposition apparatus (Method-I). The thickness of film was determined by calibration curve for the deposited amount of each compound. The film thickness can also be estimated through absorption spectral measurement (Method-II), which we have described elsewhere.[13,14] Irrespective of the employments of distinct procedures for estimation, accurate film thickness can be determined. In all systems, the thickness of PTCBI in the bilayer was constant (i.e., 160 nm) based on the Method-I. The amount of H_2Pc deposited in ITO/PTCBI/H_2Pc-A was 60 nm through the same method as PTCBI. However, since PTCBI/H_2Pc-B and PTCBI/H_2Pc-C have a fibrous structure of H_2Pc whisker (vide infra), its precise thickness was estimated through a scanning electron microscope (FE-SEM: JEOL, JSM-7000F); that is, the thicknesses of H_2Pc in PTCBI/H_2Pc-B and PTCBI/H_2Pc-C were ca. 200 and 250 nm, respectively.

Characterization. A transmission electron microscope (TEM: Hitachi, H-8000) operated at 175 kV was used to obtain a cross-sectioned bilayer image. The sample for TEM measurement was prepared by forming a bilayer on an epoxy resin (Quetol 812), according to the above-mentioned methods. Cross sections of the bilayer were cut using an ultramicrotome (Reichert–Nissei, Ultracut N) at r.t. A sample of the section was transferred to a copper microgrid (Nisshin EM) and dried at r.t. The surface of H_2Pc was observed through a FE-SEM. Absorption spectra of the fabricated bilayers were measured using a Jasco V-650 spectrophotometer. The surface roughness of H_2Pc in all the PTCBI/H_2Pc bilayers (i.e., (i) PTCBI/H_2Pc-A, (ii) PTCBI/H_2Pc-B, and (iii) PTCBI/H_2Pc-C) was measured by a laser microscope (Keyence, VK-9510). The roughness factor, calculated from the ratio of real surface area to geometrical area, was estimated to be ca. 2, 5.4, and 5 in systems (i), (ii), and (iii), respectively.

Photoelectrochemical Experiments. An electrochemical glass cell was equipped with a modified ITO working electrode (effective area: 1 × 1 cm^2), a spiral Pt counter electrode, and an Ag/AgCl (in saturated KCl electrolyte) reference electrode. The entire photoelectrochemical study was conducted in an alkaline (NaOH) solution containing a known concentration of thiol within an Ar atmosphere (pH = 10). This study was carried out using a potentiostat (Hokuto Denko, HA-301) with a function generator (Hokuto Denko, HB-104), a coulomb meter (Hokuto Denko, HF-201), and an X–Y recorder (GRAPHTEC, WX-4000) under illumination. A halogen lamp (light intensity: ca. 70 mW·cm^{-2}) was used as the light source under typical conditions. When measuring the action spectrum for the photocurrent, the lamp was used as the light source in combination with a monochromator (Soma Optics, Ltd., S-10). The calculation method of incident photon-to-current efficiency (IPCE) is given in the Supporting Information. All irradiation was conducted from the side of the ITO/PTCBI interface. Light intensity was measured using a power meter (type 3A from Ophir Japan, Ltd.).

RESULTS AND DISCUSSION

Cross sections of PTCBI/H_2Pc bilayers were observed through TEM, and typical results are shown in Figure 1. Comparing the TEM image of ITO/PTCBI/H_2Pc-A (a) with that of ITO/PTCBI/H_2Pc-B (b), in the latter, the p/n interfacial area was found to be rough due to the formation of a whiskered H_2Pc; that is, Figure 1 evidently shows that the above-mentioned thermal application resulted in an enhanced contact area of the p/n interface. Such a phthalocyanine whisker has previously been reported.[26,27] However, to the best of our knowledge, it seems that this is the first example of an organic p/n bilayer involving the whisker structure. In addition, ITO/PTCBI/H_2Pc-C (c) maintained the rough p/n interface even after further coating of H_2Pc; moreover, the H_2Pc whisker in the bilayer became thick and upright.

Furthermore, the H_2Pc surface in ITO/PTCBI/H_2Pc-A and ITO/PTCBI/H_2Pc-B was observed through SEM (Figure 2). In the ITO/PTCBI/H_2Pc-A (Figure 2a), a fine-grain morphology of H_2Pc was confirmed, while in the ITO/PTCBI/H_2Pc-B (Figure 2b), the surface of fibrous H_2Pc was observed to support the above-depicted TEM image. Figures 1 and 2 show that, particularly in the ITO/PTCBI/H_2Pc-B, the H_2Pc surface, as well as the p/n interface, had grown expansively in terms of area. The SEM image of ITO/PTCBI/H_2Pc-C is shown in Figure 2c. Further deposition of H_2Pc onto the ITO/PTCBI/H_2Pc-B under r.t. only resulted in thickening of its fibrous form. Similar to the result of TEM observation, this indicates that the p/n interface remained rough but the H_2Pc surface underwent a reformation.

All the photoelectrodes exhibited photoanodic characteristics in the presence of thiol, according to Scheme 1 (cf. those voltammograms were depicted in Figure S1, Supporting Information). The scheme also represents an energy diagram for thiol oxidation at the H_2Pc/water interface, which is drawn

dx.doi.org/10.1021/am302209b | ACS Appl. Mater. Interfaces 2013, 5, 1248–1253

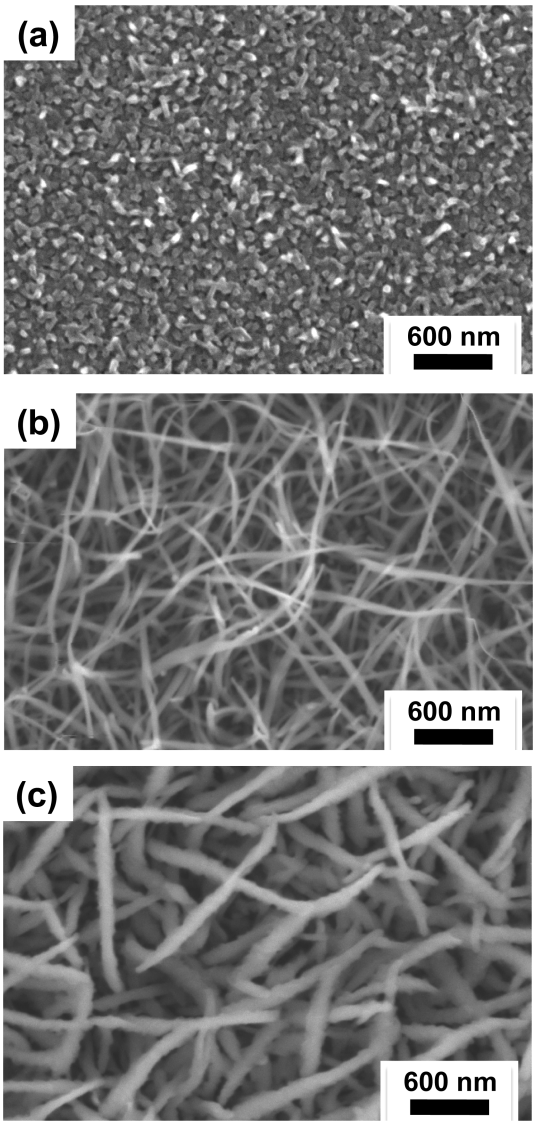

Figure 2. SEM images of H_2Pc surface in ITO/PTCBI/H_2Pc-A (a), ITO/PTCBI/H_2Pc-B (b), and ITO/PTCBI/H_2Pc-C (c).

based on the energy levels of the valence and conduction bands of the materials employed[28,29] and the oxidation potential of thiol.[17,30] The mechanistic details of thiol oxidation at the PTCBI/H_2Pc photoanode have been reported previously.[13,17]

In each system, the action spectrum for the photocurrent was measured and compared with the absorption spectrum of the bilayer employed (Figure 3a,b). Figure 3a shows that the PTCBI/H_2Pc bilayers are responsive to the entire range of visible-light energy. The magnitude of the resulting action spectra increased in the following order: ITO/PTCBI/H_2Pc-A < ITO/PTCBI/H_2Pc-B < ITO/PTCBI/H_2Pc-C. In particular, increasing IPCE values were observed in the wavelength regions at which an intense peak of H_2Pc was present. As identified from the TEM images of ITO/PTCBI/H_2Pc-B and ITO/PTCBI/H_2Pc-C (vide supra), the H_2Pc whisker grew in a vertical direction towards the surface, thus resulting in larger absorption; particularly in ITO/PTCBI/H_2Pc-C, it was due to the formation of the thick whisker of H_2Pc by its additional coating on ITO/PTCBI/H_2Pc-B. We previously reported that the action spectrum of the PTCBI/H_2Pc bilayer usually indicates that the absorption of PTCBI can mostly induce a

Scheme 1. Schematic Illustration of Oxidation at the H_2Pc/Water Interface When Applying the PTCBI/H_2Pc Bilayer to a Photoanode in the Water Phase[a]

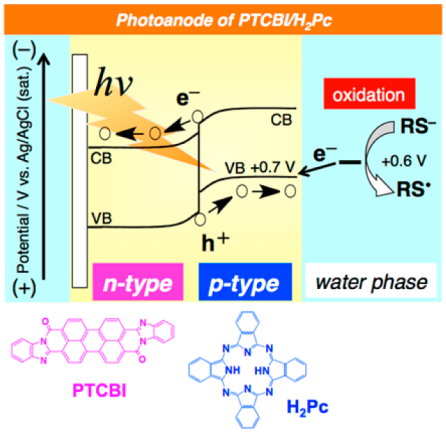

[a]Thiol is denoted as RS^-. The oxidation potential of H_2Pc (ca. +0.7 V vs. Ag/AgCl (sat.)) was electrochemically evaluated in our previous work.[17]

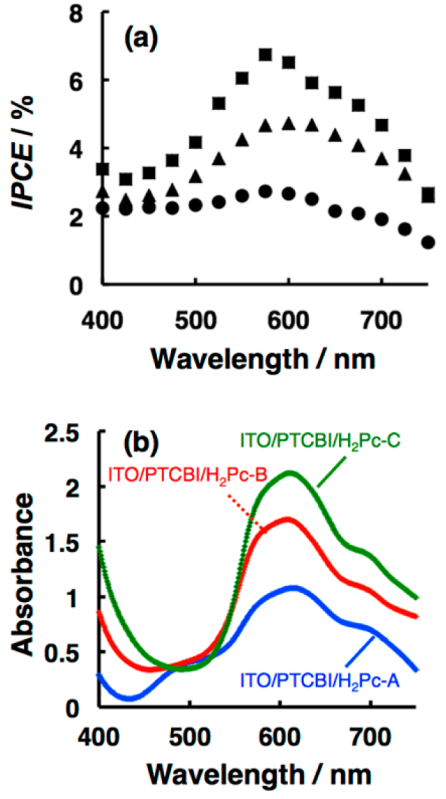

Figure 3. (a) Action spectra for photocurrent at ITO/PTCBI/H_2Pc-A (●), ITO/PTCBI/H_2Pc-B (▲), and ITO/PTCBI/H_2Pc-C (■). Concentration of thiol = 5 × 10^{-3} mol·dm^{-3} (pH = 10); applied potential = 0 V. (b) Absorption spectra of the PTCBI/H_2Pc bilayers employed for the action spectral measurements.

photocurrent generation[13,17] when employing a thick layer of PTCBI (~300 nm) under the same irradiation conditions as the present study, while there was also an evidence that the action spectrum was consistent with the transmittance spectrum of H_2Pc when irradiating light from the side of the H_2Pc/water interface in the PTCBI/H_2Pc bilayer.[13,17] The latter means little contribution of the H_2Pc absorption to

dx.doi.org/10.1021/am302209b | ACS Appl. Mater. Interfaces 2013, 5, 1248−1253

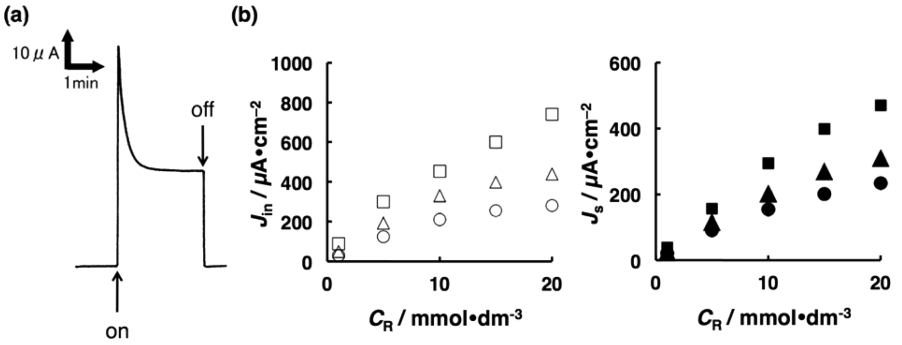

Figure 4. (a) A transient photocurrent generated at ITO/PTCBI/H_2Pc-A immediately after irradiation with white light. Light intensity = ca. 70 mW·cm^{-2}; concentration of thiol = 1×10^{-3} mol·dm^{-3} (pH = 10); applied potential = 0 V. (b) The dependencies of J_{in} (opened symbols) as well as J_s (closed symbols) on the thiol concentrations (○ and ●, ITO/PTCBI/H_2Pc-A; Δ and ▲, ITO/PTCBI/H_2Pc-B; □ and ■, ITO/PTCBI/H_2Pc-C). Light intensity and applied potential were the same as those shown in Figure 4(a).

photocurrent generation; in other words, even if the H_2Pc absorption can contribute to photocurrent generation, only H_2Pc next to the p/n interface is effective for photocurrent generation. Figure 3 may imply that, particularly in the cases of ITO/PTCBI/H_2Pc-B and ITO/PTCBI/H_2Pc-C, a rough p/n interface enables incident light to pass easily via a relatively thin layer of PTCBI (~160 nm), thus leading to an efficient absorption of H_2Pc for photocurrent generation. The more efficient action spectral characteristics of PTCBI/H_2Pc-C can be associated with the larger amount of H_2Pc neighboring to the p/n interface for an efficient absorption by H_2Pc.

The kinetic aspects of the photoelectrode characteristics of the PTCBI/H_2Pc bilayers were evaluated, and the time course of the photocurrent was measured. As a typical example, the result for ITO/PTCBI/H_2Pc-A is shown in Figure 4a. A photocurrent was observed to feature a rate-limiting charge transfer at the H_2Pc/water interface[16,17] where a spiky photocurrent (J_{in}) initially occurred, after which it attained a steady state (J_s represents a steady-state photocurrent). Furthermore, a measurement similar to that in Figure 4a was also conducted with a change in the concentration of thiol (C_R). As shown in Figure 4b, saturation in the concentration was observed for both J_{in} and J_s, supporting the conclusion that the photo-induced oxidation is not kinetically controlled by the mass transfer of thiol (i.e., diffusion). The ITO/PTCBI/H_2Pc-B and ITO/PTCBI/H_2Pc-C systems also exhibited characteristics similar to ITO/PTCBI/H_2Pc-A, and those results are also shown in Figure 4b.

Kinetics of the rate-limiting charge transfer can be analyzed assuming the Langmuir adsorption equilibrium for thiol at the H_2Pc surface. The details of the kinetic analysis have been described elsewhere[16,17,31] and are also stated in the Supporting Information. The following equations for the two types of photocurrent (J_{in} and J_s) were applied to the results of Figure 4b:

$$C_R/J_{in} = C_R/J_{max} + (k'/k)/J_{max} \quad (1)$$

$$C_R/J_s = C_R/J_{max} + \{(k'/k) + (k_f[h^*]_0/k)\}/J_{max} \quad (2)$$

where k is the rate constant of adsorption (bimolecular process), k' is the rate constant of desorption (monomolecular process), k_f is the rate constant of the electrochemical reaction, $[h^*]_0$ is the surface concentration of the hole, and J_{max} is the postulated photocurrent with maximum coverage in the occupation of all available sites. As shown in Figure 5, the linear relationships of C_R/J_{in} and C_R/J_s vs C_R showed that the

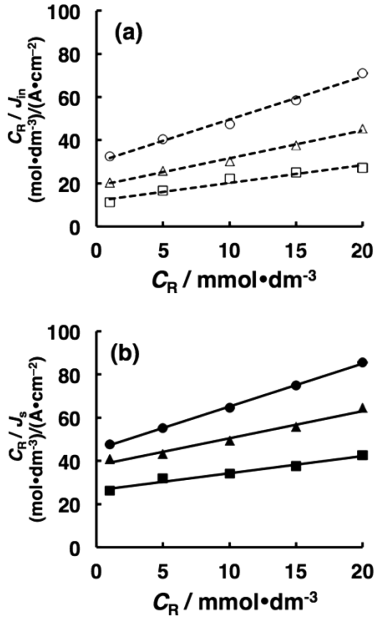

Figure 5. Plots of C_R/J_{in} and C_R/J_s vs. C_R in each system (○ and ●, ITO/PTCBI/H_2Pc-A; Δ and ▲, ITO/PTCBI/H_2Pc-B; □ and ■, ITO/PTCBI/H_2Pc-C). The kinetic parameters were obtained on the basis of eqs 1 and 2.

application of the present model to each system is valid. The resulting parameters of J_{max}, k'/k, and $k_f[h^*]_0/k$ are summarized in Table 1. The constant k'/k values are reasonable because the adsorption/desorption of thiol occurring at the H_2Pc surface should be kinetically invariable. The term $k_f[h^*]_0/k$ changed with the preparation conditions of the bilayers. Considering that the k_f and k values must be constant in all the systems studied, a variation of the $k_f[h^*]_0/k$ values can correspond to that of $[h^*]_0$. Thus, it may imply that the values of $[h^*]_0$ in the ITO/PTCBI/H_2Pc-B and ITO/PTCBI/H_2Pc-C systems are twice or more higher than that in the ITO/PTCBI/H_2Pc-A system. That is indicative of efficient light absorption and carrier generation within the p/n interior. Commonly, photocurrent (J) can be assumed to be proportional to the surface concentrations [mol·cm^{-2}] of hole (i.e., $[h^*]_0$) as well as the adsorbed thiol (Γ):

$$J \approx [h^*]_0 \times \Gamma \quad (3)$$

dx.doi.org/10.1021/am302209b | ACS Appl. Mater. Interfaces 2013, 5, 1248−1253

Table 1. Resulting Kinetic Parameters in Each PTCBI/H_2Pc System

systems	relative surface area[a] (I)	J_{max} (from J_{in}) [μA·cm^{-2}][b]	(II)	J_{max} (from J_s) [μA·cm^{-2}][b]	(III)	k'/k [mol·dm^{-3}][c]	ax (IV)	$k_f[h^*]_0/k$ [mol·dm^{-3}][d]	by (V)	relative surface concentration (Γ')[e] (VI)
ITO/PTCBI/H_2Pc-A	1.00	5.04×10^2	(1.00)	5.03×10^2	(1.00)	1.50×10^{-2}	(1.00)	7.75×10^{-3}	(1.00)	1.00
ITO/PTCBI/H_2Pc-B	2.70	7.77×10^2	(1.54)	7.96×10^2	(1.58)	1.46×10^{-2}	(1.03)	1.56×10^{-2}	(2.07)	0.76
ITO/PTCBI/H_2Pc-C	2.50	1.21×10^3	(2.40)	1.26×10^3	(2.50)	1.44×10^{-2}	(1.04)	1.87×10^{-2}	(2.51)	1.00

[a]The relative surface area was calculated considering the roughness factor (cf. the value of ITO/PTCBI/H_2Pc-A is unity). [b]The relative values of J_{max} are shown in the parentheses (cf. the value of ITO/PTCBI/H_2Pc-A is unity). [c]The inverse of k'/k (= k/k') represents the equilibrium constant for thiol adsorption at H_2Pc surface. The a values in the parentheses show the relative adsorption rate of thiol when the value of ITO/PTCBI/H_2Pc-A is unity. [d]According to the following equation, $by/ax = k_f[h^*]_0/k$, the b value in the parentheses was calculated to infer the relative oxidation rate of each system (i.e., the a and $k_f[h^*]_0/k$ values of each system, and the constant value y/x (7.75×10^{-3} for a = 1 and b =1) were introduced into the equation).[17] The relative rate corresponds to the relative value of $[h^*]_0$. [e]The relative value of J_{max} (from J_s, III) and that of $[h^*]_0$ (i.e., b value, V) were introduced into eq 3, and consequently, the Γ' value (VI) of each system was estimated.

The formal equation of eq 3 was represented as eq 1 in the Supporting Information. The relative values of surface area (from roughness factor (vide supra), I), J_{max} (from J_{in} (II) and J_s (III)), adsorption rate (IV), oxidation rate (from $k_f[h^*]_0/k$ equal to $[h^*]_0$ (vide supra) (V), and surface concentration of reactant (VI) are also listed in Table 1. The definition of these relative parameters is stated in the footnote of the table. Among the systems employed, note that in the ITO/PTCBI/H_2Pc-B system the relative value of J_{max} (II or III) is not proportional to that of $[h^*]_0$ (V); moreover, it emerges that the relative value of Γ (i.e., Γ' (VI) in Table 1) in that system is lower than that in other systems, thus resulting in an unjustifiable and low J_{max} value. The Γ' value must be essentially constant, irrespective of the systems employed in the present study. This is because surface coverage estimated from Langmuir adsorption isotherm must also be independent of the systems of H_2Pc when employing a known concentration of thiol solution. As identified from the TEM image (see Figure 1b), the H_2Pc surface can be seen to be rough in comparison with the p/n interface. That is, the deviation from unity is attributable to the difference between the p/n interfacial area and the surface area. This may originate from the formation of a thin whisker of H_2Pc particularly at the surface side. Assuming the unity of the Γ' value in the ITO/PTCBI/H_2Pc-B system, the value (i.e., 0.76) calculated from eq 3 may indicate the ratio of the p/n interfacial area to the surface area of H_2Pc (cf. the value $[h^*]_0$ should be proportional to the p/n contact area where carrier generation occurs, while J_{max} is the output at the H_2Pc surface); in other words, the original decrement of the concentration $[h^*]_0$ (V) at the surface was consequently incorporated into the Γ' value (VI) through the process of estimation (cf. the relative surface area of the B system can be estimated to multiply the b value (V) by the factor $1/\Gamma'$, thus corresponding to the value of Item I).

While a thick H_2Pc whisker formed in the ITO/PTCBI/H_2Pc-C system leading to the value of Γ' (VI) being equal to the ITO/PTCBI/H_2Pc-A system since the incremental ratio of J_{max} (II or III) between both systems is almost proportional to that of $[h^*]_0$ (V), based on the efficient photophysical events within the p/n interior, the magnitude of the oxidation kinetics at the H_2Pc/water interface was about two and a half times higher than that without thermal treatment. Furthermore, the similar relative values of Items I and V, in the ITO/PTCBI/H_2Pc-C system, may provide evidence that an increment of the p/n interfacial area is directly bound to that of the surface concentration of hole; that is, the structure of H_2Pc is nearly uniform particularly from the p/n interface to the surface.

CONCLUSION

Three types of PTCBI/H_2Pc bilayers were prepared with and without thermal application during the vapor deposition of H_2Pc. The thermal application led to the formation of a whiskered H_2Pc, thus resulting in an enhancement of the p/n interfacial area. On the basis of the action spectral measurement of the photocurrent and the kinetic analysis with the rate-limiting charge transfer at the H_2Pc/interface, it was revealed that a thick and dense whisker of H_2Pc achieves the most active oxidation through efficient photophysical events within the p/n interior. The present work shows the first example of a whiskered organic p/n bilayer compared to bulk heterojunction. The PTCBI/H_2Pc bilayer has also been recognized as a photovoltaic material in the dry state,[32] where the overall kinetics is dominated by carrier generation at the p/n interface.[23] Since the rate-limiting process in the dry cell system is considered to be much faster than the charge transfer reaction at the solid/liquid interface,[23] an organic p/n bilayer prepared by means of thermal application can lead to improved efficiency of carrier collection in a solar cell, leading to high photoenergy conversion efficiency. The organo-heterojunction material of low-molecular-weight compounds could be a promising candidate for the fabrication of practical photodevices, wherein an efficient solar cell of bulk heterojunction of a p-type porphyrin and an n-type fullerene derivative was recently found comparable to that of the p/n composite of p-type polymer in terms of efficiency.[33] As our examples of photocatalysis, when the PTCBI/H_2Pc bilayer was used in combination with an adsorbent (i.e., Nafion), it functioned as an efficient photocatalyst for the decomposition of a typical odorous compound, trimethylamine (cf., ca. 40% of EQE for CO_2 formation);[34] a photocatalysis system for H_2 evolution featuring organic p/n bilayer was also released recently, when the entire visible-light energy was available for the photocatalytic evolution of H_2.[35] Therefore, the advantageous characteristics of organic conductors (see Introduction) may open new avenues for organic photovoltaics in the dry state, as well as for photoelectrochemical and photocatalytic processes in the water phase.

■ ASSOCIATED CONTENT

Supporting Information

Calculation method of IPCE, details of kinetic analysis dealt with in the present study, and cyclic voltammograms. This material is available free of charge via the Internet at http://pubs.acs.org.

■ AUTHOR INFORMATION

Corresponding Author

*Tel/Fax: +81-172-39-3580. E-mail: tabe@cc.hirosaki-u.ac.jp.

Author Contributions

‡These authors contributed equally to this work.

Notes

The authors declare no competing financial interest.

■ ACKNOWLEDGMENTS

This work was partly supported by a Grant for Hirosaki University Institutional Research and a Grant-in-Aid for Scientific Research (T.A.) from the Ministry of Education, Culture, Sports, Science and Technology, Japan. We thank Dr. Seiji Kakuta (Aomori Prefectural Industrial Technology Research Center) for helpful assistance with the TEM and surface roughness measurements.

■ REFERENCES

(1) Tang, C. W. *Appl. Phys. Lett.* **1986**, *48*, 183−185.
(2) Wöhrle, D.; Kreienhoop, L.; Schnurpfeil, G.; Elbe, J.; Tennigkeit, B.; Hiller, S.; Schlettwein, D. *J. Mater. Chem.* **1995**, *5*, 1819−1829.
(3) Padinger, F.; Rittberger, R. S.; Sariciftci, N. S. *Adv. Funct. Mater.* **2003**, *13*, 85−88.
(4) Peet, J.; Kim, J. Y.; Coates, N. E.; Ma, W. L.; Moses, D.; Heeger, A. J.; Bazan, G. C. *Nat. Mater.* **2007**, *6*, 497−500.
(5) Bottari, G.; de la Torre, G.; Guldi, D. M.; Torres, T. *Chem. Rev.* **2010**, *110*, 6768−6816.
(6) Sun, Y.; Welch, G. C.; Leong, W. L.; Takacs, C. J.; Bazan, G. C.; Heeger, A. J. *Nat. Mater.* **2012**, *11*, 44−48.
(7) Kido, J.; Kimura, M.; Nagai, K. *Science* **1995**, *267*, 1332−1334.
(8) Suk, J.; Wu, Z.; Wang, L.; Bard, A. J. *J. Am. Chem. Soc.* **2011**, *133*, 14675−14685.
(9) Lu, L.-P.; Kabra, D.; Johnson, K.; Friend, R. H. *Adv. Funct. Mater.* **2012**, *22*, 144−150.
(10) Crone, B.; Dodabalapur, A.; Lin, Y.-Y.; Filas, R. W.; Bao, Z.; LaDuca, A.; Sarpeshkar, R.; Katz, H. E.; Li, W. *Nature* **2000**, *403*, 521−523.
(11) McCarthy, M. A.; Liu, B.; Donoghue, E. P.; Kravchenko, I.; Kim, D. Y.; So, F.; Rinzler, A. G. *Science* **2011**, *332*, 570−573.
(12) Lee, S. S.; Loth, M. A.; Anthony, J. E.; Loo, Y.-L. *J. Am. Chem. Soc.* **2012**, *134*, 5436−5439.
(13) Abe, T.; Nagai, K.; Kaneko, M.; Okubo, T.; Sekimoto, K.; Tajiri, A.; Norimatsu, T. *ChemPhysChem* **2004**, *5*, 716−720.
(14) Abe, T.; Nagai, K.; Ogiwara, T.; Ogasawara, S.; Kaneko, M.; Tajiri, A.; Norimatsu, T. *J. Electroanal. Chem.* **2006**, *587*, 127−132.
(15) Abe, T.; Nagai, K.; Kabutomori, S.; Kaneko, M.; Tajiri, A.; Norimatsu, T. *Angew. Chem., Int. Ed.* **2006**, *45*, 2778−2781.
(16) Abe, T.; Nagai, K.; Ichinohe, H.; Shibata, T.; Tajiri, A.; Norimatsu, T. *J. Electroanal. Chem.* **2007**, *599*, 65−71.
(17) Abe, T.; Miyakushi, S.; Nagai, K.; Norimatsu, T. *Phys. Chem. Chem. Phys.* **2008**, *10*, 1562−1568.
(18) Zhang, S.; Sakai, R.; Abe, T.; Iyoda, T.; Norimatsu, T.; Nagai, K. *ACS Appl. Mater. Interfaces* **2011**, *3*, 1902−1909.
(19) Abe, T.; Nakamura, K.; Ichinohe, H.; Nagai, K. *J. Mater. Sci.* **2012**, *47*, 1071−1076.
(20) Abe, T.; Nagai, K.; Sekimoto, K.; Tajiri, A.; Norimatsu, T. *Electrochem. Commun.* **2005**, *7*, 1129−1132.
(21) Abe, T.; Tobinai, S.; Nagai, K. *Jpn. J. Appl. Phys.* **2009**, *48*, 021503.
(22) Abe, T.; Tobinai, S.; Taira, N.; Chiba, J.; Itoh, T.; Nagai, K. *J. Phys. Chem. C* **2011**, *115*, 7701−7705.
(23) Oekermann, T.; Schlettwein, D.; Wöhrle, D. *J. Appl. Electrochem.* **1997**, *27*, 1172−1178.
(24) Mihailetchi, V. D.; Wildeman, J.; Blom, P. W. M. *Phys. Rev. Lett.* **2005**, *94*, 126602.
(25) Maki, T.; Hashimoto, H. *Bull. Chem. Soc. Jpn.* **1952**, *25*, 411−413.
(26) Lee, Y.-L.; Tsai, W.-C.; Maa, J.-R. *Appl. Surf. Sci.* **2001**, *173*, 352−361.
(27) Liu, C. J.; Shih, J. J.; Ju, Y. H. *Sens. Actuators, B: Chem.* **2004**, *99*, 344−349.
(28) Peumans, P.; Bulovíc, V.; Forrest, S. R. *Appl. Phys. Lett.* **2000**, *76*, 2650−2652.
(29) Suemori, K.; Miyata, T.; Yokoyama, M.; Hiramoto, M. *Appl. Phys. Lett.* **2005**, *86*, 063509.
(30) Surdhar, S.; Armstrong, D. A. *J. Phys. Chem.* **1986**, *90*, 5915−5917.
(31) Kermann, E.; Schlettwein, D.; Jaeger, N. I. *J. Electroanal. Chem.* **1996**, *405*, 149−158.
(32) Hiramoto, M.; Fukusumi, H.; Yokoyama, M. *Appl. Phys. Lett.* **1992**, *61*, 2580−2582.
(33) Matsuo, Y.; Sato, Y.; Niinomi, T.; Soga, I.; Tanaka, H.; Nakamura, E. *J. Am. Chem. Soc.* **2009**, *131*, 16048−16050.
(34) Nagai, K.; Abe, T.; Kaneyasu, Y.; Yasuda, Y.; Kimishima, I.; Iyoda, T.; Imaya, H. *ChemSusChem* **2011**, *4*, 727−730.
(35) Abe, T.; Chiba, J.; Ishidoya, M.; Nagai, K. *RSC Adv.* **2012**, *2*, 7992−7796.